

# Learning from Feedback: Semantic Enhancement for Object SLAM Using Foundation Models

Jungseok Hong<sup>1</sup>, Ran Choi<sup>1</sup>, John J. Leonard<sup>1</sup>

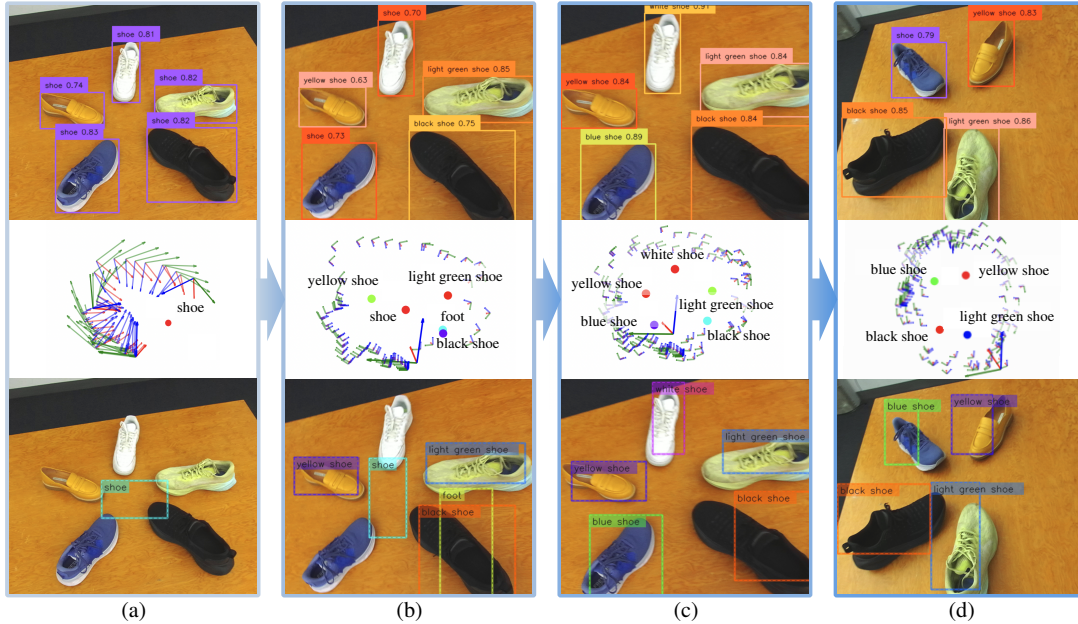


Fig. 1: Demonstration of SEO-SLAM’s semantic mapping capabilities. (a) Initial mapping with generic labels. (b) Detection with descriptive labels from the MLLM feedback and building maps with more landmarks. (c) Estimated semantic map with all the shoes associated successfully. (d) Updated semantic map after scene change (white shoe removed). Top row: Object detection results; Middle row: Estimated semantic maps; Bottom row: Landmarks projected onto camera frames to be used as the MLLM’s input. This sequence illustrates *SEO-SLAM’s* ability to refine object labels, update maps in cluttered environments, and adapt to scene changes.

**Abstract**—Semantic Simultaneous Localization and Mapping (SLAM) systems struggle to map semantically similar objects in close proximity, especially in cluttered indoor environments. We introduce Semantic Enhancement for Object SLAM (SEO-SLAM), a novel SLAM system that leverages Vision-Language Models (VLMs) and Multimodal Large Language Models (MLLMs) to enhance object-level semantic mapping in such environments. SEO-SLAM tackles existing challenges by (1) generating more specific and descriptive open-vocabulary object labels using MLLMs, (2) simultaneously correcting factors causing erroneous landmarks, and (3) dynamically updating a multiclass confusion matrix to mitigate object detector biases. Our approach enables more precise distinctions between similar objects and maintains map coherence by reflecting scene changes through MLLM feedback. We evaluate SEO-SLAM on our challenging dataset, demonstrating enhanced accuracy and robustness in environments with multiple similar objects. Our system outperforms existing approaches in terms of landmark matching accuracy and semantic consistency. Results show the feedback from MLLM improves object-centric semantic mapping. Our dataset is publicly available at: [jungseokhong.com/SEO-SLAM](http://jungseokhong.com/SEO-SLAM).

## I. INTRODUCTION

Simultaneous Localization and Mapping (SLAM) has evolved from focusing on geometric accuracy to integrating semantic information, enhancing its utility for downstream tasks such as navigation [1], manipulation [2], and planning [3]. This evolution aligns with advances in computer vision and deep learning [4], introducing richer and more accurate environmental representations. Recent developments in foundation models, such as large language models (LLM) [5]–[7], vision language models (VLM) [8], [9], and multimodal LLM (MLLM) [10], [11], have shown that they can extract semantic information from data in an open-vocabulary setting. Several studies [12]–[20] show that the foundation models can perform spatial reasoning from a given scene or map with semantic features embedded. Beyond mapping, [21], [22] present semantic SLAM using the foundation models.

Despite these advances, critical challenges persist in semantic SLAM: (1) Distinguishing between similar objects in close proximity remains difficult when detectors only provide generic labels (*e.g.*, “shoe” for all shoes). This results in the fusion of similar objects into a single landmark, as

<sup>1</sup> The authors are with the Computer Science and Artificial Intelligence Laboratory (CSAIL) at the Massachusetts Institute of Technology (MIT), 32 Vassar St, Cambridge, MA 02139, USA. Corresponding author: Jungseok Hong ([jungseok@mit.edu](mailto:jungseok@mit.edu))

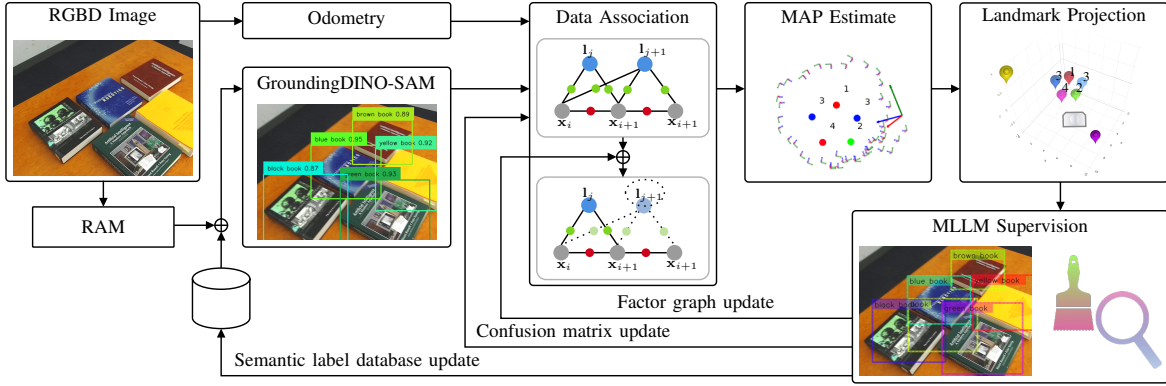


Fig. 2: Overview of the SEO-SLAM system: The pipeline begins with an RGBD image input, from which odometry is derived. RAM processes the RGB image to generate object tag lists. GroundingDINO and SAM then localize and segment objects based on these tags. Geometric and semantic information from the RGBD image and odometry are fed into a factor graph. MAP estimation is obtained through factor graph optimization. Landmarks from the current map are projected onto the camera frame and overlaid on the image. This composite image is used as input for MLLM, which provides feedback on each landmark based on the current scene. The MLLM’s feedback is used to update: (1) the semantic label database for GroundingDINO, (2) the multiclass prediction confusion matrix, and (3) the list of erroneous factors. For example, if the feedback informs  $I_{j+1}$  is an erroneous landmark, factors related to  $I_{j+1}$  are removed.

shown in (Fig 1a). (2) Erroneous landmarks pose a significant challenge in maintaining consistent maps over time. This issue can be caused by sensor measurement uncertainties or scene changes, particularly in cluttered and dynamic environments. (3) Object detectors are vulnerable to inherent biases in their training datasets, causing consistent semantic errors in some objects.

To address these challenges, we aim to leverage foundation models’ semantic understanding and SLAM’s spatial accuracy to build maps that are both semantically and spatially consistent. Foundation models have robust semantic understanding capabilities, but limited spatial reasoning without a prebuilt map with embedded semantic features. Conversely, SLAM systems excel at capturing spatial information, but often struggle with maintaining reliable semantic information. By combining these strengths, we propose Semantic Enhancement for Object SLAM (SEO-SLAM), a novel approach that leverages VLM and MLLM for semantic SLAM (Fig 2). The main contributions of our work include:

- 1) Integrating image tagging, tag-based grounding, and segmentation models into the SLAM pipeline to enable descriptive open-vocabulary object detection and refine semantic information of landmarks.
- 2) Harnessing MLLMs for generating more descriptive labels for existing landmarks and rectifying erroneous landmarks to reduce perceptual aliasing.
- 3) Presenting a method to use MLLM responses to update a multiclass prediction confusion matrix and identify duplicated landmarks.
- 4) Experimental results demonstrating the improved object semantic mapping accuracy in challenging scenarios with multiple similar objects in close proximity.
- 5) Introducing datasets which have semantically similar objects in a single scene with odometry, ground truth trajectory data, and ground truth object information.

## II. RELATED WORK

Semantic SLAM extends traditional SLAM by incorporating semantic information into the mapping and localization process. Since the early work of Galindo *et al.* [23], semantic SLAM has benefited from advances in deep learning and computer vision [24]. Recent systems like Kimera [25], EAO-SLAM [26], and DSP-SLAM [27] have demonstrated improved performance in various environments. However, these systems often struggle with dynamic objects and distinguishing between semantically similar objects.

Some approaches, like [28] and [29], have attempted to address the challenge of dynamic objects by incorporating prior knowledge about those objects. Several object-centric SLAM approaches, such as [26], [30], [31], have focused on improving object-level mapping accuracy. These methods primarily evaluate their performance based on the quantity of objects correctly mapped. However, they are generally limited to closed-set object scenes and lack evaluation of semantic accuracy, particularly in distinguishing between similar objects or handling precise classification.

Data association is crucial for handling perceptual aliasing and maintaining map consistency in SLAM. Early works addressed this with approaches such as joint compatibility [32], probabilistic data association [33], multiple hypothesis [34]. As semantic SLAM has emerged, data association techniques that use semantic information have been introduced. Bowman *et al.* [35] proposed an Expectation-Maximization (EM) algorithm-based approach to jointly optimize landmark position and semantics. Utilizing mixture models [36], Doherty *et al.* [37] coupled geometric (continuous) and semantic (discrete) information of landmarks for optimization, where they show that a mixture approach outperforms the EM-based approach. Bernreiter *et al.* [38] developed a multiple hypothesis approach with an optimizing hypothesis tree. However, these methods are often limited to closed-set se-

mantics or require prior knowledge of a multiclass prediction confusion matrix.

The recent advances in foundation models [39] and open-vocabulary detection [40] have advanced semantic SLAM such as ConceptGraphs [21] and LEXIS [22]. Gu *et al.* [21] focus on building a semantic map embedding multimodal features for various downstream tasks. Kassab *et al.* [22] show how open-vocabulary language models can be integrated into SLAM systems to enhance semantic understanding. However, the challenges in semantic SLAM introduced in Section I still remain an open problem.

Our proposed SEO-SLAM utilizes the factor graph framework GTSAM [41], uniquely harnessing VLM and MLLM to generate contextually richer object labels for a consistent semantic map, dynamically update a multiclass confusion matrix, and correct erroneous landmarks. With this approach, we aim to address the limitations of existing semantic SLAM systems, particularly in environments with multiple similar objects, and enable more accurate and robust mapping.

### III. METHOD

SLAM can be defined as finding a set of robot poses  $\mathbf{x}$  and landmark positions  $\mathbf{l}$  given a set of measurements  $\mathbf{z}$ . This can be formulated as a maximum prior (MAP) problem, and  $\hat{X}, \hat{L}$  represent the estimated robot poses and landmark positions.

$$\hat{X}, \hat{L} = \arg \max_{X, L} p(X, L | Z) \quad (1)$$

where  $X = \{\mathbf{x}_i \in SE(3)\}, i \in \{0, 1, \dots, N\}$  and  $L = \{\mathbf{l}_j \in \mathbb{R}^3\}, j \in \{0, 1, \dots, M\}$ .

SEO-SLAM aims to solve this MAP problem while incorporating rich semantic information. To accommodate open-vocabulary semantics, we optimize the MAP problem using only geometric information while leveraging the connection between semantic and geometric information from our measurements. This is achieved by fusing semantic information from our detector and depth images. Our approach can handle open-vocabulary semantic classes without requiring prior knowledge of class prediction statistics for a multiclass prediction confusion matrix. Fig 2 shows the overall architecture of our SEO-SLAM pipeline. Each component of the pipeline is explained in the following sections.

#### A. Geometric and Semantic Data Association

For data association, we start with a measurement model in Eq 2 where  $\mathbf{v}_{ij}$  is a normal disbution with zero-mean and  $\Gamma$  covariance, and  $\mathbf{z}_{ij}$  is the predicted measurement of landmark  $\mathbf{l}_j$  at a robot pose  $\mathbf{x}_i$ .

$$\mathbf{z}_{ij} := h_{ij}(\mathbf{x}) + \mathbf{v}_{ij} \quad (2)$$

Given the model and a measurement  $\mathbf{z}_k$ , we aim to determine the probability  $P(\mathbf{z}_k, j_k = j | Z^-)$  that we can associate the measurement  $\mathbf{z}_k$  to a landmark  $j$ , considering all previous measurements  $Z^-$ . This probabilistic formulation allows us to quantify the likelihood of measurement-landmark associations based on the previous observations. As derived in [42], this probability can be connected to SLAM with a state vector  $\mathbf{x}$  as shown in Eq 3 where  $C_{i_k j}$  is the covariance

TABLE I: Notations for Algorithm 1

Notation	Description
E: Empty	The bounding box contains no relevant object.
IC: Incorrect	The landmark is misclassified or misplaced.
R <sub>IC</sub> : Refined	The landmark class label is updated from an incorrect label.
C: Correct	The landmark classification is correct.
D: Duplicated	Multiple bounding boxes refer to the same landmark.
P: Precise among Duplicated	Indicates the most accurate class label among duplicates.
G: Generated	Generated descriptive labels from generic labels.
$\mathcal{M}$ : Multiclass confusion matrix	Confusion matrix for multiclass prediction
$\mathcal{D}$ : Duplicates confusion matrix	Confusion matrix for duplicates and precise labels

#### Algorithm 1 MLLM Supervision for Landmark Refinement

```

1: Input: Composite image  $I$ , Landmarks' labels  $T$ 
2: Output: Landmark factors to refine
3: procedure MLLM_LANDMARK_SUPERVISION( $I, T$ )
4:   for  $l_j, t_j$  in  $I, T$  do  $S_j = \mathbf{LandmarkEval}(l_j, t_j)$ 
5:     if  $S_j \in \text{IC}$  then
6:       Return factors related to  $l_j$ .
7:       Update  $\mathcal{M}$  with  $\{\text{IC}, \text{R}_{\text{IC}}\}$  pair.
8:     else if  $S_j \in \text{D-P}$  then
9:       Return factors related to  $l_j$ .
10:      Update  $\mathcal{D}$  with  $\{\text{D}, \text{P}\}$  pair.
11:     else if  $S_j \in \text{E}$  then
12:       Return factors related to  $l_j$ .
13:     else if  $S_j \in \text{C} \cup \text{P}$  then
14:        $G = \mathbf{ClassLabelGen}(l_j)$ 
15:     end if
16:   end for
17: end procedure

```

\* $l_j$ : landmark,  $t_j$ : landmark label

and  $\Sigma$  is subset covariance matrix between the landmark  $\mathbf{l}_j$  and the robot pose  $\mathbf{x}_i$ .

$$P(\tilde{\mathbf{z}}_k, j_k = j | Z^-) = \int_{\mathbf{x}} P(\tilde{\mathbf{z}}_k, j_k = j | \mathbf{x}) P(\mathbf{x} | Z^-) \approx \frac{1}{\sqrt{|2\pi C_{i_k j}|}} e^{-\frac{1}{2} \|\mathbf{h}_{i_k j}(\tilde{\mathbf{x}}) - \tilde{\mathbf{z}}_k\|_{C_{i_k j}}^2} \quad (3)$$

$$C_{i_k j} := \frac{\partial \mathbf{h}_{i_k j}}{\partial \mathbf{x}} \Big|_{\tilde{\mathbf{x}}} \Sigma \frac{\partial \mathbf{h}_{i_k j}}{\partial \mathbf{x}} \Big|_{\tilde{\mathbf{x}}}^T + \Gamma \quad (4)$$

From the measurement likelihood in Eq 5 and current state estimate in Eq 6, the approximation in Eq 3 is derived.

$$P(\tilde{\mathbf{z}}_k, j_k = j | \mathbf{x}) = \frac{1}{\sqrt{|2\pi \Gamma|}} e^{-\frac{1}{2} \|\mathbf{h}_{i_k j}(\mathbf{x}) - \tilde{\mathbf{z}}_k\|_{\Gamma}^2} \quad (5)$$

$$P(\mathbf{x} | Z^-) = \frac{1}{\sqrt{|2\pi \Sigma|}} e^{-\frac{1}{2} \|\mathbf{x} - \hat{\mathbf{x}}\|_{\Sigma}^2} \quad (6)$$

By taking negative logarithm on Eq 3, we can obtain Eq 7 for a chi-square test [42]. We use this to determine if there is a significant association between a given landmark and

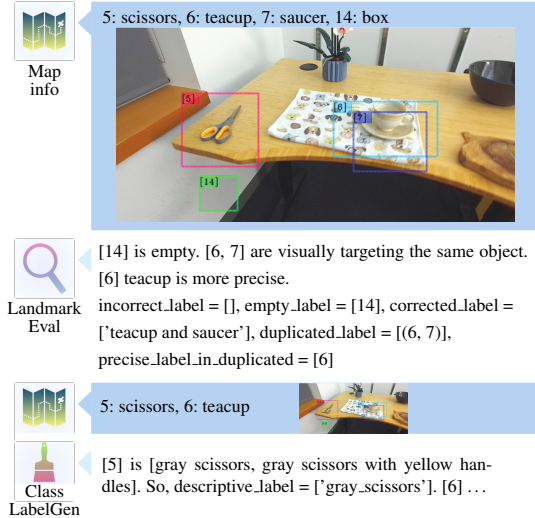


Fig. 3: Example Feedback from the MLLMs: MapInfo provides an RGB image with landmarks projected from the 3D semantic map, along with the label of each landmark. *LandmarkEval* inspects the objects within the given bounding boxes and their labels, eliminating incorrect landmarks. *ClassLabelGen* generates descriptive labels for the remaining landmarks based on their distinctive visual features.

measurements.

$$D_{k,j}^{2,ML} := \|\mathbf{h}_{ikj}(\hat{x}) - \tilde{\mathbf{z}}_k\|_{C_{ikj}}^2 < \chi_{d,\alpha}^2 \quad (7)$$

where  $d$  is the dimension of a measurement and  $\alpha$  is confidence level.

Following the chi-square test, we conduct a semantic similarity assessment for each measurement against the given landmark. This process involves extracting word embedding vectors for both measurement and landmark labels, then calculating their cosine similarity. This word embedding-based semantic measure is crucial for enabling an open-vocabulary setting in our pipeline, allowing us to handle class labels unknown prior to deployment. We apply a predefined similarity threshold to filter the measurements, adding those exceeding this threshold as hypotheses for the landmarks.

### B. Object Detection

We use the RAM-Grounded-SAM (RGS) [43] for object detection, which combines three models: (1) Recognize-Anything Model (RAM) [44], an open-set tagging model, (2) GroundingDINO [45], a grounding model for object detection, and (3) Segment-Anything Model (SAM) [46] a segmentation model. The advantage of this approach is that RGS’s integrated pipeline allows us to incorporate object labels derived from the MLLM. Additionally, leveraging GroundingDINO’s strong zero-shot capabilities enables our system to distinguish semantically similar objects in close proximity using descriptive labels, which are generated based on each object’s distinctive features.

### C. MLLM Supervision for Refining Landmarks

While Grounded-SAM is effective in capturing objects using tags from RAM, classes recognized with this ap-

proach are mostly generic semantic categories (e.g., book, car, shoes), which need to be more descriptive to register separate landmarks where objects are in close proximity. To address this issue, we propose an MLLM-based supervision algorithm for landmark refinement, outlined in Algorithm 1 where notations are in Table I. Specifically, we harness two MLLMs for landmark evaluation (*LandmarkEval*) and class label generation (*ClassLabelGen*) with structured, step-by-step prompts for efficient execution [47], [48].

Overlaying prompts directly on an image is known to enhance MLLM’s understanding, making the model more effective at identifying target objects compared to text-based descriptions or coordinate inputs [49], [50]. Therefore, we first process the current semantic map into a composite image  $I$  and store its landmarks’ labels  $T$  with the following steps to use  $\{I, T\}$  as inputs. (1) Map Projection: Project 3D landmarks onto the current camera frame, and (2) Bounding Box Generation: Create bounding boxes for each landmark based on object dimensions and current camera pose, and (3) Landmark Overlay: Combine the current RGB image with projected landmark bounding boxes to create  $I$ . Additionally, we display a number assigned to each landmark at the corner of the bounding boxes (Fig 3). This is to ensure better recognition of each landmark by the MLLM, as numbers are more recognizable than text and to avoid text being obscured. Cropped images corresponding to each bounding box are also provided to assist more accurate visual identification.

With the inputs, *LandmarkEval* evaluate landmarks in  $I$  to refine them by (1) identifying objects that have disappeared from the scene, (2) detecting incorrectly labeled objects and correcting them, and (3) finding duplicate landmark labels (e.g., toy, figure, and doll referring to a single object) and selecting the most appropriate label. *ClassLabelGen* then creates descriptive labels for correctly labeled landmarks using their colors. This approach is based on our preliminary experiments, which showed that GroundingDINO can distinguish objects better when additional color information is provided. The newly generated labels are then added to the semantic label database. While RAM outputs generic tags, our method transforms these into more detailed and descriptive labels. These labels improve GroundingDINO’s ability to separately capture similar objects in close proximity.

### D. Confusion Matrix for Improving Semantics

We update our confusion matrices  $\mathcal{M}$  and  $\mathcal{D}$  using feedback  $\{\text{IC}, \text{R}_{\text{IC}}\}$  and  $\{\text{D}, \text{P}\}$  (Algorithm 1, Table I) while allowing them to dynamically resize as we use open-vocabulary semantic labels and keeping descriptive labels non-deterministic.  $\mathcal{M}$  is utilized to update predictions from our detection model. For each detection class  $c$  from RGS, we employ its confidence score as a prior for the class  $c$  and estimate posteriors using Eq 8 (for class  $c$ ) and Eq 9 (for the others), where  $N$  is the number of classes in  $\mathcal{M}$ . The class prediction is then updated to the one with the highest estimated probability.

$$P(c|\mathcal{M}) \propto P(c) P(\mathcal{M}|c) \quad (8)$$

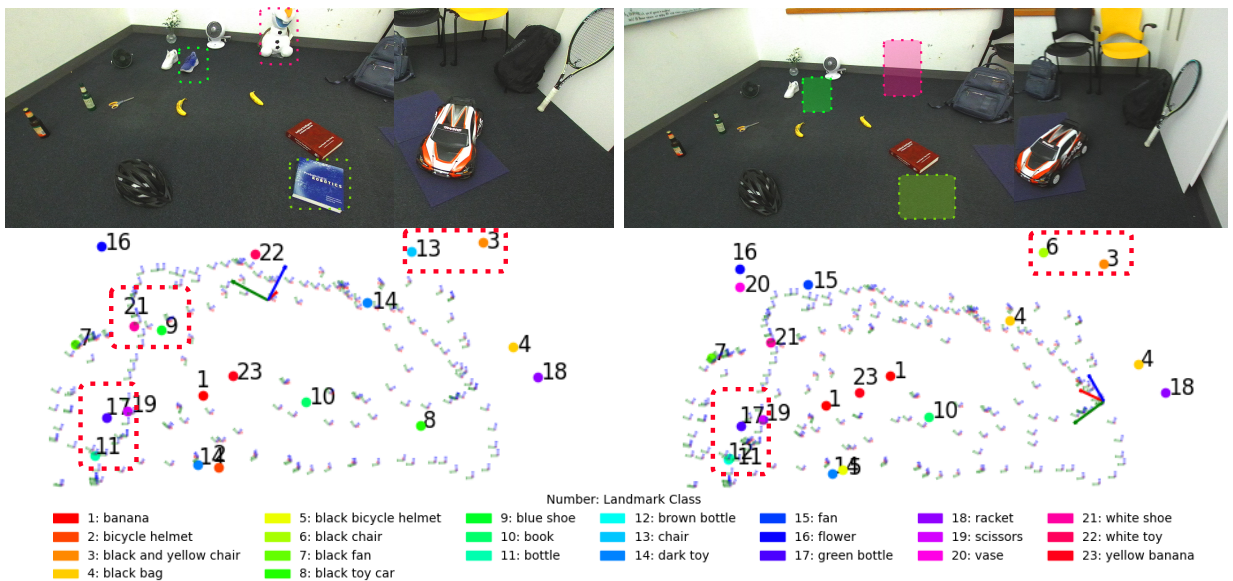


Fig. 4: Qualitative Results from the MD1 Dataset. The top images show the scene changes where the blue shoe, snowman, and blue book are removed. Note that SEO-SLAM separates objects in close proximity (e.g., shoes (9, 21), bottles (11, 17), and chairs (3, 6, 13)) and removes the blue shoe (9). However, the system only captures one book from the scene.

$$P(\bar{c}|\mathcal{M}) \propto \frac{1 - P(c)}{N - 1} \times P(\mathcal{M}|\bar{c}) \quad (9)$$

Additionally, we use  $\mathcal{D}$  to proactively remove duplicate landmarks. Potential duplicates are identified when landmark bounding boxes overlap by more than 90% and when the distance between landmarks is less than 0.1m. In this case,  $\mathcal{D}$  is used to check the semantic similarity between these landmarks, and the one with a generic label is removed. This approach not only reduces our pipeline’s execution time but also improves the accuracy of the MLLM by decreasing the number of landmark queries in the composite image  $I$ .

#### IV. EXPERIMENTAL SETUP AND RESULTS

##### A. Data Collection

We collected six datasets in indoor room environments containing everyday objects (Table II). We categorized the datasets as small ( $\approx 10$ ), medium ( $\approx 20$ ), or large ( $\approx 30$ ) based on the number of objects present. We used a ZED2i stereo camera to collect RGB images and odometry data. Ground truth trajectory was captured using an OptiTrack motion capture system. To create challenging scenarios, objects of the same category were placed in close proximity.

##### B. Experiments Setup

We employ the RAM++ large model (plus\_swin\_large) for image tagging and filter out tags that are overly and do not represent a single objects (e.g., sit, white, many objects). Object grounding is handled by the GroundingDINO large model (swinb\_cogcoor), while segmentation tasks are performed using SAM with a ViT-H model. In our RGS model, we set the confidence threshold to 0.5 and the GroundingDINO IoU threshold to 0.5. For the MLLMs, we utilize the ChatGPT API (gpt-4o version) with default settings for

TABLE II: Summary of Object Datasets\*

Dataset	Objects
Small 1 (11)	bag, banana, book, chair, fan, flower, helmet, scissors, shoe, racquet, vase
Small 2 (11)	banana, bin, book, chair, fan, flower, football, scissors, snowman, teacup, vase
Medium 1 (21)	bag (2), banana (2), book (2), bottle (2), chair (2), fan (2), flower, helmet, racquet, scissors, shoe (2), snowman, toy car, vase
Medium 2 (20)	banana (2), bin (2), book (2), chair (2), cup, fan, flower, football, helmet, scissors, shoe, snowman, teacup (2), racquet, vase
Large 1 (32)	bag, banana (3), bin (3), book (3), bottle (2), chair (3), cup, fan, flower, football, helmet, monitor (3), electric outlet, racquet, scissors, shoe (2), snowman, teacup (2), vase
Large 2 (30)	apple (2), bag, banana (4), bin (2), book, bowl, chair (2), Cheez-It box (2), electric outlet, fan, flower, football (2), hammer (2), helmet, racquet, scissors, shoes(3), teacup, vase

(\* ) indicates the number of objects

both *LandmarkEval* and *ClassLabelGen* and execute them asynchronously to optimize our system speed.

We conducted experiments with the six datasets (Table II). Our evaluation metrics include the semantic accuracy of landmarks, the number of false landmarks, and Absolute Pose Error (APE). We compared three methods: our SEO-SLAM approach, which uses RGS as the object detector with MLLM-based feedback for landmark refinement; RGS alone, which uses RAM-Grounded-SAM for open-vocabulary detection without MLLM feedback; and YOLO (baseline), using pre-trained YOLO v8 for object detection. This experimental setup allowed us to comprehensively assess both semantic mapping performance and trajectory

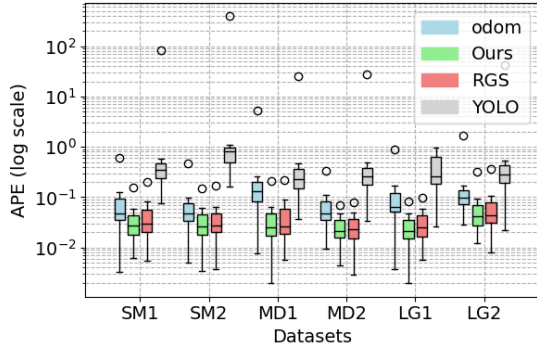


Fig. 5: Absolute Pose Error (APE) evaluation results across our six datasets with three methods compared to odometry on a logarithmic scale. Open circles represent outliers.

accuracy across different datasets and methods in open-vocabulary settings.

### C. Results

Table III shows a comprehensive comparison of semantic mapping performance between ours, RGS, and YOLO across six datasets of varying complexity. The results demonstrate that ours consistently outperforms the other methods in terms of semantic accuracy and estimating the number of landmarks. In most datasets, ours achieves the highest precision and F1 scores, indicating improvements in semantic accuracy from feedback. This is particularly evident in SM1, MD1, and LG2, where ours maintains consistent performance while RGS and YOLO show degradation. Notably, ours generally produces fewer false positive landmarks than the other methods, demonstrating improved robustness in our cluttered environments. The robust performance of ours can be attributed to its ability to leverage MLLM feedback for refining landmark descriptions and reducing perceptual aliasing. However, in LG1, ours shows similar performance to RGS since there are more objects in each frame, which degrades the quality of the feedback from the MLLM. Overall, the results demonstrate the effectiveness of SEO-SLAM in improving semantic mapping accuracy and reducing false positives across various environmental complexities.

We also evaluate the trajectory errors of each method compared to odometry (Fig 5). Ours consistently shows a lower median APE than the others across all the datasets. RGS also performs well, with low median errors and fewer outliers than YOLO. YOLO shows the highest median errors and outliers because YOLO can only detect objects in the training dataset. This demonstrates that our open-vocabulary detector is more robust and accurate across diverse conditions. Fig 4 presents qualitative results from the MD1 Dataset. SEO-SLAM successfully distinguishes between objects in close proximity and shows its capability to update the semantic map in response to scene changes. While SEO-SLAM captures most objects, it sometimes struggles when objects are too close. For instance, it only maps one book in the scene.

TABLE III: Semantic Mapping Evaluation Results\*

Dataset	Method	Semantic Acc.			Num. of Landmarks	
		P	R	F1	Est.	False Pos.
SM1	<b>Ours</b>	<b>0.79</b>	<b>1.00</b>	<b>0.88</b>	14	3
	RGS	0.52	<b>1.00</b>	0.69	21	10
	YOLO	0.26	0.73	0.38	31	23
SM2	<b>Ours</b>	<b>0.47</b>	0.64	<b>0.54</b>	15	8
	RGS	0.39	<b>0.82</b>	0.53	23	14
	YOLO	0.17	<b>0.82</b>	0.29	52	43
MD1	<b>Ours</b>	<b>0.73</b>	<b>0.76</b>	<b>0.74</b>	22	6
	RGS	0.45	0.71	0.56	33	18
	YOLO	0.35	0.71	0.47	43	28
MD2	<b>Ours</b>	<b>0.68</b>	0.85	<b>0.76</b>	25	8
	RGS	0.56	<b>0.95</b>	0.70	34	15
	YOLO	0.37	0.70	0.48	38	24
LG1	<b>Ours</b>	0.71	<b>0.78</b>	<b>0.75</b>	35	10
	RGS	<b>0.79</b>	0.72	<b>0.75</b>	29	6
	YOLO	0.35	0.56	0.43	52	34
LG2	<b>Ours</b>	<b>0.66</b>	<b>0.70</b>	<b>0.68</b>	32	11
	RGS	0.35	0.63	0.45	54	35
	YOLO	0.31	0.53	0.40	51	35

\*P: Precision, R: Recall, F1: F-1 score, Est.: the number of estimated landmarks, False Pos.: the number of false positive landmarks

### D. Limitations

While SEO-SLAM shows significant improvements in semantic mapping, it is important to acknowledge some limitations. We found the MLLM in SEO-SLAM struggles to generate non-color-based distinctive labels from objects in the same category with similar colors in close proximity. Additionally, its performance is sensitive to environmental lighting conditions, which can affect its color-based object identification performance. In the future, we plan to address these issues by enabling MLLM to generate labels from distinctive features of objects via meta prompting.

## V. CONCLUSIONS

We present SEO-SLAM, a novel approach to object SLAM that leverages the semantic understanding capabilities of foundation models to enhance object-level semantic mapping in cluttered indoor environments. By incorporating feedback from the MLLMs, SEO-SLAM addresses key challenges in existing semantic SLAM systems. With feedback, it generates more descriptive open-vocabulary object labels, simultaneously corrects those factors that cause spurious landmarks, and dynamically updates a multiclass confusion matrix. The experimental results demonstrate that SEO-SLAM consistently outperforms baseline methods across datasets of varying complexity, improving semantic accuracy, landmark estimation, and trajectory accuracy. This approach is particularly capable of reducing false positive landmarks and improving robustness in environments with multiple similar objects. Thus, SEO-SLAM represents a significant step forward in combining the semantic understanding capabilities of foundation models with the spatial accuracy of SLAM systems. This paper opens up new avenues for more accurate and robust semantic mapping in complex and dynamic environments.

## REFERENCES

- [1] H. Temeltas and D. Kayak, "Slam for robot navigation," *IEEE Aerospace and Electronic Systems Magazine*, vol. 23, no. 12, pp. 16–19, 2008.
- [2] J. Peng, X. Shi, J. Wu, and Z. Xiong, "An object-oriented semantic slam system towards dynamic environments for mobile manipulation," in *2019 IEEE/ASME International Conference on Advanced Intelligent Mechatronics (AIM)*. IEEE, 2019, pp. 199–204.
- [3] Y. Hasegawa and Y. Fujimoto, "Experimental verification of path planning with slam," *IEEE Journal of Industry Applications*, vol. 5, no. 3, pp. 253–260, 2016.
- [4] C. Cadena, L. Carlone, H. Carrillo, Y. Latif, D. Scaramuzza, J. Neira, I. Reid, and J. J. Leonard, "Past, present, and future of simultaneous localization and mapping: Toward the robust-perception age," *IEEE Transactions on robotics*, vol. 32, no. 6, pp. 1309–1332, 2016.
- [5] H. Touvron, T. Lavril, G. Izacard, X. Martinet, M.-A. Lachaux, T. Lacroix, B. Rozière, N. Goyal, E. Hambro, F. Azhar, et al., "Llama: Open and efficient foundation language models," *arXiv preprint arXiv:2302.13971*, 2023.
- [6] A. Q. Jiang, A. Sablayrolles, A. Mensch, C. Bamford, D. S. Chaplot, D. d. l. Casas, F. Bressand, G. Lengyel, G. Lample, L. Saulnier, et al., "Mistral 7b," *arXiv preprint arXiv:2310.06825*, 2023.
- [7] T. B. Brown, "Language models are few-shot learners," *arXiv preprint arXiv:2005.14165*, 2020.
- [8] M. Caron, H. Touvron, I. Misra, H. Jégou, J. Mairal, P. Bojanowski, and A. Joulin, "Emerging properties in self-supervised vision transformers," in *Proceedings of the IEEE/CVF international conference on computer vision*, 2021, pp. 9650–9660.
- [9] A. Radford, J. W. Kim, C. Hallacy, A. Ramesh, G. Goh, S. Agarwal, G. Sastry, A. Askell, P. Mishkin, J. Clark, et al., "Learning transferable visual models from natural language supervision," in *International conference on machine learning*. PMLR, 2021, pp. 8748–8763.
- [10] H. Liu, C. Li, Q. Wu, and Y. J. Lee, "Visual instruction tuning," *Advances in neural information processing systems*, vol. 36, 2024.
- [11] W. Dai, J. Li, D. Li, A. M. H. Tiong, J. Zhao, W. Wang, B. Li, P. Fung, and S. Hoi, "Instructblip: towards general-purpose vision-language models with instruction tuning," in *Proceedings of the 37th International Conference on Neural Information Processing Systems*, ser. NIPS '23. Red Hook, NY, USA: Curran Associates Inc., 2024.
- [12] T. Salzmann, M. Ryll, A. Bewley, and M. Minderer, "Scene-graph vit: End-to-end open-vocabulary visual relationship detection," *arXiv preprint arXiv:2403.14270*, 2024.
- [13] B. Chen, Z. Xu, S. Kirmani, B. Ichter, D. Sadigh, L. Guibas, and F. Xia, "Spatialvlm: Endowing vision-language models with spatial reasoning capabilities," in *Proceedings of the IEEE/CVF Conference on Computer Vision and Pattern Recognition*, 2024, pp. 14 455–14 465.
- [14] R. Fu, J. Liu, X. Chen, Y. Nie, and W. Xiong, "Scene-llm: Extending language model for 3d visual understanding and reasoning," *arXiv preprint arXiv:2403.11401*, 2024.
- [15] G. Chen, L. Shen, R. Shao, X. Deng, and L. Nie, "Lion: Empowering multimodal large language model with dual-level visual knowledge," in *Proceedings of the IEEE/CVF Conference on Computer Vision and Pattern Recognition*, 2024, pp. 26 540–26 550.
- [16] M. Tie, J. Wei, Z. Wang, K. Wu, S. Yuan, K. Zhang, J. Jia, J. Zhao, Z. Gan, and W. Ding, "O2v-mapping: Online open-vocabulary mapping with neural implicit representation," *arXiv preprint arXiv:2404.06836*, 2024.
- [17] Y. Deng, J. Wang, J. Zhao, X. Tian, G. Chen, Y. Yang, and Y. Yue, "Opengraph: Open-vocabulary hierarchical 3d graph representation in large-scale outdoor environments," *arXiv preprint arXiv:2403.09412*, 2024.
- [18] J. Kerr, C. M. Kim, K. Goldberg, A. Kanazawa, and M. Tancik, "Lerf: Language embedded radiance fields," in *Proceedings of the IEEE/CVF International Conference on Computer Vision*, 2023, pp. 19 729–19 739.
- [19] S. Linok, T. Zemskova, S. Ladanova, R. Titkov, and D. Yudin, "Beyond bare queries: Open-vocabulary object retrieval with 3d scene graph," *arXiv preprint arXiv:2406.07113*, 2024.
- [20] S. Matsuzaki, T. Sugino, K. Tanaka, Z. Sha, S. Nakaoka, S. Yoshizawa, and K. Shintani, "Clip-loc: Multi-modal landmark association for global localization in object-based maps," *arXiv preprint arXiv:2402.06092*, 2024.
- [21] Q. Gu, A. Kuwajerwala, S. Morin, K. M. Jatavallabhula, B. Sen, A. Agarwal, C. Rivera, W. Paul, K. Ellis, R. Chellappa, et al., "Conceptgraphs: Open-vocabulary 3d scene graphs for perception and planning," in *2024 IEEE International Conference on Robotics and Automation (ICRA)*. IEEE, 2024, pp. 5021–5028.
- [22] C. Kassab, M. Mattamala, L. Zhang, and M. Fallon, "Language-extended indoor slam: a versatile system for real-time visual scene understanding," in *2024 IEEE International Conference on Robotics and Automation (ICRA)*. IEEE, 2024, pp. 15 988–15 994.
- [23] C. Galindo, A. Saffiotti, S. Coradeschi, P. Buschka, J.-A. Fernandez-Madrigo, and J. González, "Multi-hierarchical semantic maps for mobile robotics," in *2005 IEEE/RSJ international conference on intelligent robots and systems*. IEEE, 2005, pp. 2278–2283.
- [24] K. Chen, J. Zhang, J. Liu, Q. Tong, R. Liu, and S. Chen, "Semantic visual simultaneous localization and mapping: A survey," *arXiv preprint arXiv:2209.06428*, 2022.
- [25] A. Rosinol, M. Abate, Y. Chang, and L. Carlone, "Kimera: an open-source library for real-time metric-semantic localization and mapping," in *2020 IEEE International Conference on Robotics and Automation (ICRA)*. IEEE, 2020, pp. 1689–1696.
- [26] Y. Wu, Y. Zhang, D. Zhu, Y. Feng, S. Coleman, and D. Kerr, "Eao-slam: Monocular semi-dense object slam based on ensemble data association," in *2020 IEEE/RSJ International Conference on Intelligent Robots and Systems (IROS)*. IEEE, 2020, pp. 4966–4973.
- [27] J. Wang, M. Rünz, and L. Agapito, "Dsp-slam: Object oriented slam with deep shape priors," in *2021 International Conference on 3D Vision (3DV)*. IEEE, 2021, pp. 1362–1371.
- [28] C. Yu, Z. Liu, X.-J. Liu, F. Xie, Y. Yang, Q. Wei, and Q. Fei, "Dslam: A semantic visual slam towards dynamic environments," in *2018 IEEE/RSJ international conference on intelligent robots and systems (IROS)*. IEEE, 2018, pp. 1168–1174.
- [29] L. Xiao, J. Wang, X. Qiu, Z. Rong, and X. Zou, "Dynamic-slam: Semantic monocular visual localization and mapping based on deep learning in dynamic environment," *Robotics and Autonomous Systems*, vol. 117, pp. 1–16, 2019.
- [30] A. Iqbal and N. R. Gans, "Localization of classified objects in slam using nonparametric statistics and clustering," in *2018 IEEE/RSJ International Conference on Intelligent Robots and Systems (IROS)*. IEEE, 2018, pp. 161–168.
- [31] A. Adkins, T. Chen, and J. Biswas, "Obvi-slam: Long-term object-visual slam," *IEEE Robotics and Automation Letters*, 2024.
- [32] J. Neira and J. D. Tardós, "Data association in stochastic mapping using the joint compatibility test," *IEEE Transactions on robotics and automation*, vol. 17, no. 6, pp. 890–897, 2001.
- [33] Y. Bar-Shalom and E. Tse, "Tracking in a cluttered environment with probabilistic data association," *Automatica*, vol. 11, no. 5, pp. 451–460, 1975. [Online]. Available: <https://www.sciencedirect.com/science/article/pii/0005109875900217>
- [34] D. Reid, "An algorithm for tracking multiple targets," *IEEE transactions on Automatic Control*, vol. 24, no. 6, pp. 843–854, 1979.
- [35] S. L. Bowman, N. Atanasov, K. Daniilidis, and G. J. Pappas, "Probabilistic data association for semantic slam," in *2017 IEEE International Conference on Robotics and Automation (ICRA)*, 2017, pp. 1722–1729.
- [36] E. Olson and P. Agarwal, "Inference on networks of mixtures for robust robot mapping," *The International Journal of Robotics Research*, vol. 32, no. 7, pp. 826–840, 2013.
- [37] K. J. Doherty, D. P. Baxter, E. Schneeweiss, and J. J. Leonard, "Probabilistic data association via mixture models for robust semantic slam," in *2020 IEEE International Conference on Robotics and Automation (ICRA)*, 2020, pp. 1098–1104.
- [38] L. Bernreiter, A. Gawel, H. Sommer, J. Nieto, R. Siegwart, and C. C. Lerma, "Multiple hypothesis semantic mapping for robust data association," *IEEE Robotics and Automation Letters*, vol. 4, no. 4, pp. 3255–3262, 2019.
- [39] OpenAI and J. A. et al., "Gpt-4 technical report," 2024. [Online]. Available: <https://arxiv.org/abs/2303.08774>
- [40] A. Zareian, K. D. Rosa, D. H. Hu, and S.-F. Chang, "Open-vocabulary object detection using captions," in *Proceedings of the IEEE/CVF Conference on Computer Vision and Pattern Recognition*, 2021, pp. 14 393–14 402.
- [41] M. Kaess, H. Johannsson, R. Roberts, V. Ila, J. J. Leonard, and F. Dellaert, "isam2: Incremental smoothing and mapping using the bayes tree," *The International Journal of Robotics Research*, vol. 31, no. 2, pp. 216–235, 2012.
- [42] M. Kaess and F. Dellaert, "Covariance recovery from a square root information matrix for data association," *Robotics and autonomous systems*, vol. 57, no. 12, pp. 1198–1210, 2009.

- [43] T. Ren, S. Liu, A. Zeng, J. Lin, K. Li, H. Cao, J. Chen, X. Huang, Y. Chen, F. Yan, *et al.*, “Grounded sam: Assembling open-world models for diverse visual tasks,” *arXiv preprint arXiv:2401.14159*, 2024.
- [44] X. Huang, Y.-J. Huang, Y. Zhang, W. Tian, R. Feng, Y. Zhang, Y. Xie, Y. Li, and L. Zhang, “Inject semantic concepts into image tagging for open-set recognition,” *arXiv preprint arXiv:2310.15200*, 2023.
- [45] S. Liu, Z. Zeng, T. Ren, F. Li, H. Zhang, J. Yang, C. Li, J. Yang, H. Su, J. Zhu, *et al.*, “Grounding dino: Marrying dino with grounded pre-training for open-set object detection,” *arXiv preprint arXiv:2303.05499*, 2023.
- [46] A. Kirillov, E. Mintun, N. Ravi, H. Mao, C. Rolland, L. Gustafson, T. Xiao, S. Whitehead, A. C. Berg, W.-Y. Lo, *et al.*, “Segment anything,” in *Proceedings of the IEEE/CVF International Conference on Computer Vision*, 2023, pp. 4015–4026.
- [47] J. Wei, X. Wang, D. Schuurmans, M. Bosma, F. Xia, E. Chi, Q. V. Le, D. Zhou, *et al.*, “Chain-of-thought prompting elicits reasoning in large language models,” *Advances in neural information processing systems*, vol. 35, pp. 24 824–24 837, 2022.
- [48] Z. Zhang, A. Zhang, M. Li, and A. Smola, “Automatic chain of thought prompting in large language models,” *arXiv preprint arXiv:2210.03493*, 2022.
- [49] J. Yang, H. Zhang, F. Li, X. Zou, C. Li, and J. Gao, “Set-of-mark prompting unleashes extraordinary visual grounding in gpt-4v,” *arXiv preprint arXiv:2310.11441*, 2023.
- [50] Z. Yang, L. Li, K. Lin, J. Wang, C.-C. Lin, Z. Liu, and L. Wang, “The dawn of lmms: Preliminary explorations with gpt-4v (ision),” *arXiv preprint arXiv:2309.17421*, vol. 9, no. 1, p. 1, 2023.